Draft version 1.0

ATLAS NOTE

October 12, 2009

Minimizing the TileCal correlated noise effect: a simple approach

M.C.N. Fiolhais[a] and A. Onofre[a]

[a] *LIP, Departamento de Física da Universidade de Coimbra*

Abstract

The TileCal noise in the high gain read-out is investigated in this note. Apart from the dominant and intrinsic white noise component, a correlated contribution between different TileCal channels is observed. This affects and degrades the response of the calorimeter. In this note the correlated noise component is studied and a simple method, based on a χ^2 minimization, is proposed to parametrize the response of the photomultipliers. Using data from TileCal pedestal runs it is shown that the correlated noise component can be significantly reduced and mostly removed. The need for a double Gaussian distribution, which typically describes the noise behaviour of the TileCal cannot, however, be fully ruled out after removing the correlated noise component within a module. This suggests that the double Gaussian distribution of TileCal pedestals is not only related to the correlated noise itself within the module but has a different source which requires further investigation.

1 Introduction

The ATLAS detector [1] is a general purpose detector which was designed to fully exploit the physics potential of the Large Hadron Collider (LHC). The final configuration of the experiment reflected the stringent constraints imposed by the LHC parameters i.e., proton-proton collisions at a centre-of-mass energy of 14 TeV, with a design luminosity of $10^{34}\mathrm{cm}^{-2}\mathrm{s}^{-1}$ and bunch crossing every 25 ns. The ATLAS experiment is composed of inner detectors, calorimeters (electromagnetic and hadronic) and muon spectrometers. The inner detectors are embeded in a 2T solenoid magnetic field. Three toroidal magnets are used in addition for the muon system.

Electromagnetic and hadronic calorimeters are fundamental for a general purpose hadron collider detector as ATLAS, once they must provide accurate energy and position measurements of electrons, photons, isolated hadrons, jets and transverse missing energy. They also help on particle identification and in particular on muon momentum reconstruction. The Tile Calorimeter (TileCal) [2], the main focus of this note, is a hadronic sampling calorimeter using iron as absorber and scintillating plastic plates (designated by *tiles*) as active material. It has a novel geometry of alternating layers, perpendicular to the beam direction, radially staggered in depth, and has a cylindrical structure divided into three cylindrical sections: the barrel (B) and the two extended barrels (EB). Each of the three sections is divided into 64 azimuthal segments, referred as modules, with $\Delta\phi = 2\pi/64 \sim 0.1$. The light produced by particles when crossing the TileCal *tiles* is read out from two sides by wavelength shifting (WLS) fibres which are bundled together to form readout cells with three different sampling depths. Each cell is read out by two photomultipliers (PMTs), one at each side. With a total of 4672 readout cells, the TileCal comprises approximately 10000 PMTs in the entire calorimeter. The TileCal was designed to have good time resolution ($\sim$1 ns) and a typical granularity of $\Delta\eta \times \Delta\phi = 0.1 \times 0.1$ (0.1×0.2 for the last layer) in order to achieve good jet energy and missing transverse energy resolutions.

This note is organized as follows. After the introduction, a short description of the TileCal structure is given in Section 2 and in Section 3 evidence for correlated noise between TileCal PMT's (within a given module) is shown. In Section 4 the χ^2 method used to unfold the correlated noise component is described, and results of applying the method to the TileCal noise in the high gain read-out mode are presented in Section 5. Conclusions are discussed at the end in Section 6.

2 The TileCal cells layout

The grouping of the TileCal WLS fibers to specific PMT's allows the segmentation of the modules in η and radial depth which implies an almost projective tower structure of the TileCal. The barrel covers the $|\eta| < 1.0$ region and is contained in a single cylinder with separate partitions for positive and negative η. Two partitions of the Extended-Barrel (EB), which covers $0.8 < |\eta| < 1.7$, are contained in a cylinder. The four partitions are named LBA, LBC, EBA and EBC, where A(C) corresponds to positive (negative) values of η. The TileCal has 3 sampling layers (A, BC and D). In Figure 1, the layout of the cells is shown.

The barrel and EB modules contain 90 and 32 PMTs, respectively, placed in metallic cases called drawers. For each barrel module, there are 2 drawers and each one can allocate 48 PMTs. Three of these are empty. For the EB, modules can host only one drawer with 38 PMTs with 6 empty slots. Each TileCal PMT signal is processed by fast and low noise read-out front-end electronics near the detector. Signals are then transmitted via optical links to off-detector back-end electronics and during the process undesirable effects, like cross talk, may happen between different PMT signals [4]. This will result in a correlated noise pattern between different channels which may have a negative impact on the TileCal performances, like the reconstructed jet energy resolution. In the following the correlated noise effect in the TileCal is studied using high gain pedestal runs, and a simple method is applied to remove this

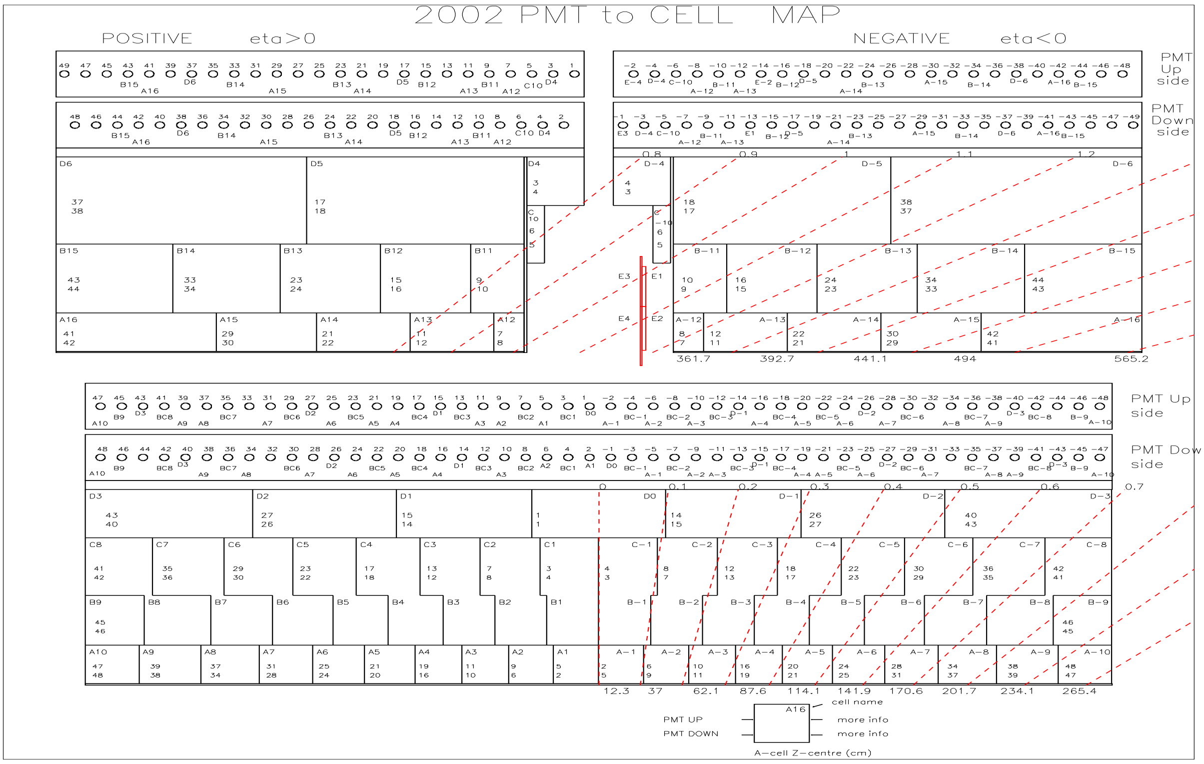

Figure 1: Cells and tile-rows of the hadronic calorimeter TileCal.

undesirable effect. As the proof of principle is the major concern of the current note, only few modules of the TileCal were surveyed. A large scale systematic study is still to be performed.

3 The TileCal correlated noise

To estimate how signals from two different PMTs (x_i and x_j) within the same TileCal module, with corresponding mean values $\mu_i = E[x_i]$ and $\mu_j = E[x_j]$ are correlated, it is adequate to evaluate the covariance between the two channels

$$\mathbf{cov}(x_i, x_j) \quad = \quad E[(x_i - \mu_i)(x_j - \mu_j)] = < x_i x_j > - \mu_i \mu_j, \tag{1}$$

where the operator E denotes expected values. The extension to the full set of channels within the specific TileCal module is straightforward. The resulting covariance matrix can then provide usefull information about how the signal from a specific channel is determined by the signal in any other channel. The correlation matrix, defined according to

$$\rho(x_i, x_j) \quad = \quad \frac{\mathbf{cov}(x_i, x_j)}{\sqrt{E[(x_i - \mu_i)^2]}\sqrt{E[(x_j - \mu_j)^2]}} = \frac{\mathbf{cov}(x_i, x_j)}{\sigma_i . \sigma_j}, \tag{2}$$

is also very useful. In Figure 2 a) the covariance matrix, in (ADC counts)^2, is represented for the TileCal module LBA23, using 10000 events from the high gain pedestal run 125204. Regions of high and low covariance values are clearly visible. In Figure 2 b) a two dimensional plot shows the pedestal data of PMT 35 as a function of the pedestal of PMT 10. No correlation whatosever seem to be present between these two channels. This effect can clearly be seen also in the covariance plot. For Figure 2 c) and Figure 2 d) the situation changes and a clear correlation between the noise distributions of the PMTs is visible. The data also suggests that even in the case where the correlated noise could be completely removed, the intrinsic white noise distribution (the dominant contribution) of each one of these channels seems to have a larger RMS than the pedestal distribution which, for instance, characterize the response of PMT 10. In Figure 3 a double Gaussian fit, centered at zero,

$$P(x_i) \quad = \quad P_0 e^{-0.5.P_1.x_i^2} + P_2 e^{-0.5.P_3.x_i^2}, \tag{3}$$

is applied to the pedestal distributions of PMT 10 and PMT 48, before removing the correlated noise component. The standard deviation (σ) of each normal distribution can be obtained by evaluating $\sqrt{1/P_1}$ and $\sqrt{1/P_3}$. Two comments are appropriate. The first one relates to what was already stressed above i.e., the standard deviation of the dominant Gaussian for PMT 10 is smaller than for PMT 48 which suggests that PMT 48 is intrinsically noisier than PMT 10. The other one is related to the fact that a fit with only one Gaussian distribution would result in a worst χ^2 even in the case of PMT 10. This fact suggests that the need for a double Gaussian distribution may not be completely determined by the correlations between the different channels within the module, but has an additional source which needs further investigation. This behaviour was observed also for other PMTs of the LBA23 module and other modules of the TileCal.

4 The χ^2 method

To address the problem of the correlated noise in the TileCal it is desirable to consider a general approach based on first principles which do not depend on the specific source of the problem, once it is not known at the moment. If the method proves correct, it should enhance the properties of any correlations and give insight to possible solutions. The approach presented in this note considers that the observed noise measurement (x_i) in a particular PMT i of the TileCal module, is a combination of a genuine intrinsic noise component (x_i^{int}) plus a contribution which depends on the response of all PMTs in the module as a whole and it is probably dominated by the closest neighbours. The simplest approach to reconstruct the measurement in PMT channel i is then to consider x_i as beeing a linear combination between the intrinsic noise component (x_i^{int}) and a weighted sum of the signals of all the other PMTs (N_{PMT}) in the module i.e.,

$$x_i \quad = \quad x_i^{int} + \sum_{j \neq i}^{N_{PMT}} \alpha_{i,j} x_j. \tag{4}$$

The $\alpha_{i,j}$ unknown parameters make sure measurements from other PMTs are taken into account with different weights, task left to the method to figure out. One less trivial approximation can also be considered: if the method works well in case of dealing with noise (which is the case of this note) one may assume the intrinsic noise distribution itself (the PMT pedestals) will be narrower after correcting any undesirable effects approaching ideally to a delta function with a mean around zero ($x_i^{int} \sim 0$). One may think, given the fact that calibrated values are used in the measurements, that signal offsets (represented by β_i) may be present and should be taken into account to compensate for effects that deviates the intrinsic mean value of the channel from zero (like miscalibrations). In this case the previous expression turns into

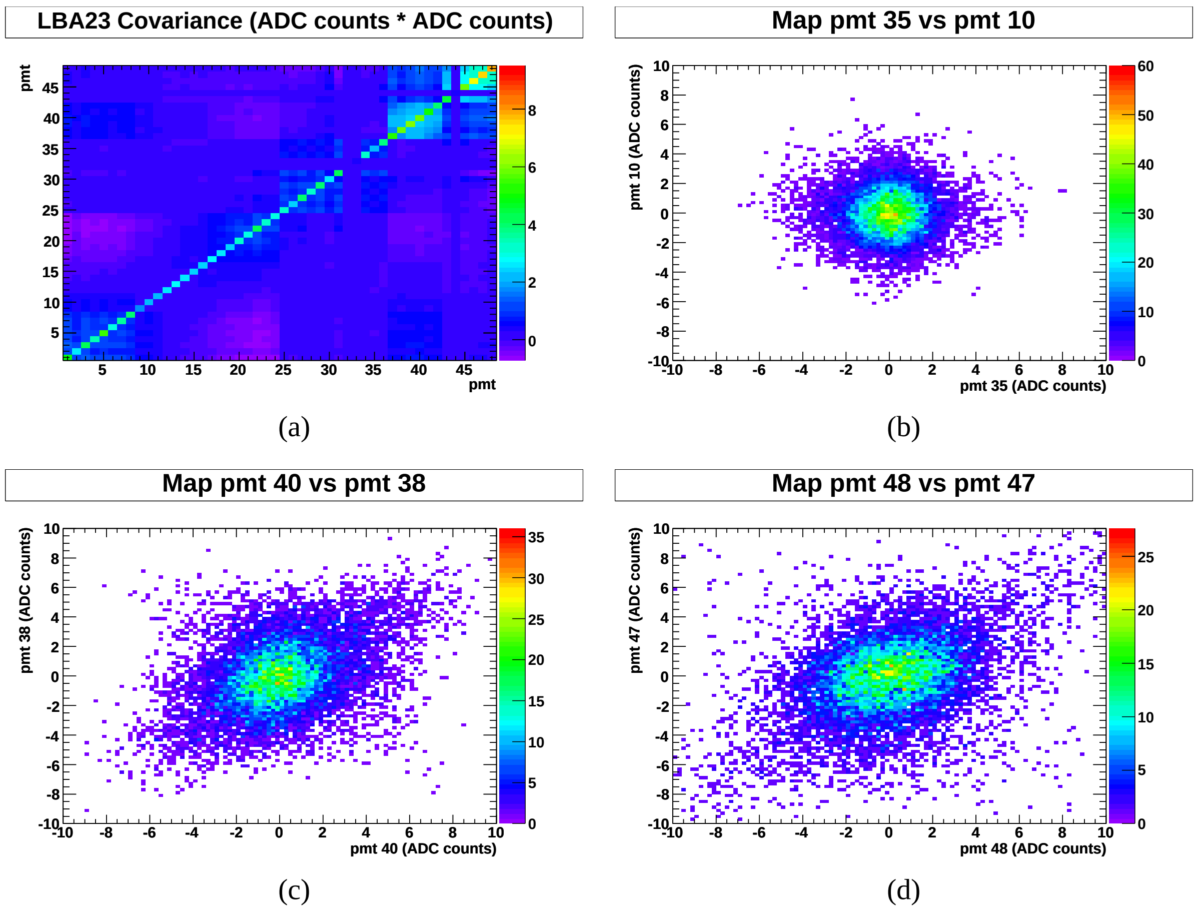

Figure 2: a) The two dimensional covariance matrix, in (ADC counts)^2, is represented for the LBA23 module of the TileCal. In b) the response of PMT 35 is represented against the one from PMT 10. In c) the response of PMT 40 is represented against PMT 38 and in d) the response of PMT 48 is represented against PMT 47.

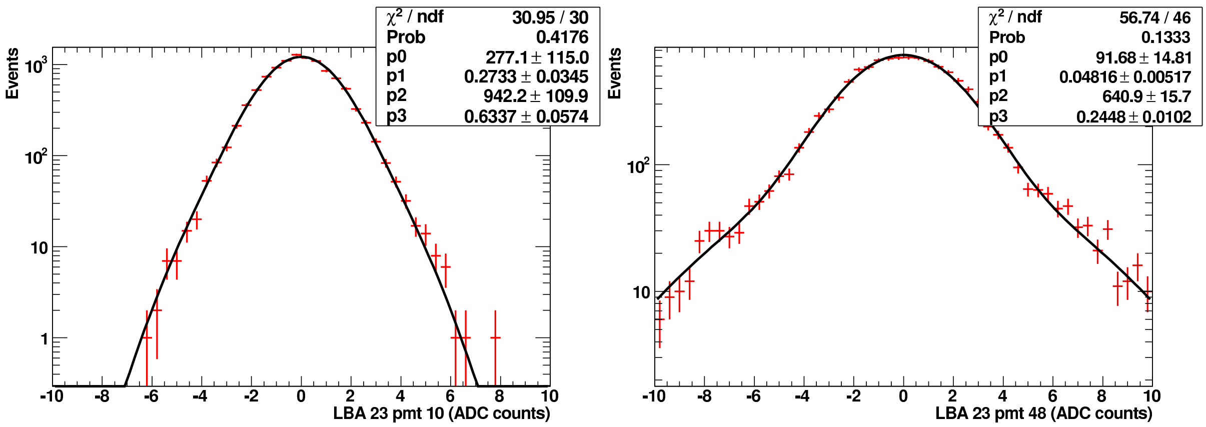

Figure 3: The double Gaussian fit to the pedestal distribution of PMT 10 (left) and PMT 48 (right) is shown.

$$\begin{aligned}
x_1 &\sim \beta_1 + \alpha_{1,2}x_2 + ... + \alpha_{1,N_{PMT}}x_{N_{PMT}} \\
x_2 &\sim \alpha_{2,1}x_1 + \beta_2, + ... + \alpha_{2,N_{PMT}}x_{N_{PMT}} \\
&. \\
&. \\
&. \\
x_{N_{PMT}} &\sim \alpha_{N_{PMT},1}x_1 + \alpha_{N_{PMT},2}x_2 + ... + \beta_{N_{PMT}}
\end{aligned} \tag{5}$$

Obviously these hypothesis will be tested when the offset β_i and correlated noise contribution ($\sum_{k\neq i}\alpha_{i,k}x_k$) will be subtracted from the measured values of each PMT x_i, in order to obtain the intrinsic PMT signal.

For each channel, the measured signal can be compared with the model above using the usual χ^2 method,

$$\chi_i^2 = \sum_{Events} \frac{\left[x_i - (\beta_i + \sum_{k\neq i}^{N_{PMT}} \alpha_{i,k}x_k)\right]^2}{\sigma_i^2}, \tag{6}$$

which can be minimized (individualy for each PMT channel) with respect to each one of the $\alpha_{i,j}$ and β_i of the model,

$$\frac{\partial\chi_i^2}{\partial\alpha_{i,1}} = \frac{\partial\chi_i^2}{\partial\alpha_{i,2}} = ... = \frac{\partial\chi_i^2}{\partial\alpha_{i,N_{PMT}}} = \frac{\partial\chi_i^2}{\partial\beta_i} = 0. \tag{7}$$

Following the minimization procedure, the α matrix

$$\begin{pmatrix} 0 & \alpha_{1,2} & ... & \alpha_{1,N_{PMT}} \\ \alpha_{2,1} & 0 & ... & \alpha_{2,N_{PMT}} \\ ... & ... & ... & ... \\ \alpha_{N_{PMT},1} & \alpha_{N_{PMT},2} & ... & 0 \end{pmatrix}$$

is obtained together with the offsets β_i for each one of the channels. The reconstruction of the signal in channel i (x_i^{rec}) is performed removing the offset evaluated during the minimization procedure β_i and by applying the α matrix to the measured values of all the other PMTs of the module according to,

$$x_i^{rec} = x_i - (\alpha_{i,1}x_1 + \alpha_{i,2}x_2 + ... + \beta_i + ... + \alpha_{i,N_{PMT}}x_{N_{PMT}}) \tag{8}$$

The reconstructed signal x_i^{rec} should describe the intrinsic noise component (x_i^{int}) of channel i with mean around zero for each of the PMTs. Any deviation should be regarded as a limitation of this simplistic approach.

5 Results

As a proof of principle, the χ^2 method described in the previous section was applied to the TileCal LBA23 module. Although several other modules were also tested with similar results (described at the end of this section), a systematic survey of the full TileCal is still to be performed. In Figure 4 the two dimensional covariance matrices before and after applying the χ^2 method are shown. The correlated noise component seem to be significantly reduced after applying the method.

In Figure 5 the noise (pedestal) from PMT 47 is plotted against the one from PMT 46 before (left) and after (right) removing the correlated noise component with the χ^2 method. While for Figure 5 (left) the measured values x_i were used, in Figure 5 (right) the reconstructed values x_i^{rec} were applied. A clear improvement is observed i.e., the correlation between both PMTs are very much reduced after applying the χ^2 method. In Figure 6 the same distributions are shown for PMT 35 versus PMT 10 before and after removing the correlated noise component. As can be seen, when no correlations are observed between PMTs before applying the χ^2 method, the signals remain uncorrelated after applying the method. To first approximation the method is performing as expected: it recovers the signals from PMTs which are correlated by removing the observed correlation and preserves the signals of non correlated channels.

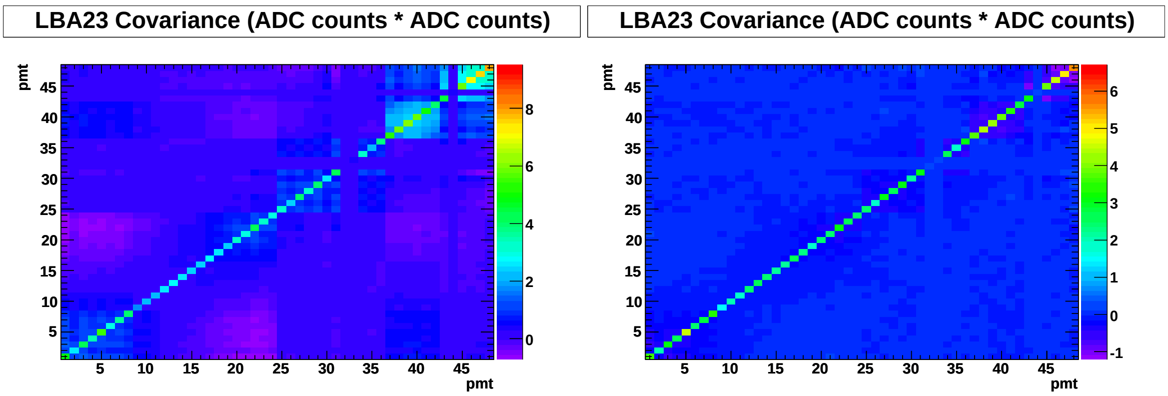

Figure 4: The two dimensional covariance matrix, in (ADC counts)^2, is represented for the LBA23 before (left) and after (right) removing the correlated noise component.

It should also be stressed that, after applying the method, all PMT signals show a decrease of the distribution RMS as can be seen in Figure 7. The top (red) and bottom (blue) lines of Figure 7 (left) correspond to the values obtained before and after applying the χ^2 method, respectively. Figure 7 (right) shows the relative change of the RMS as a function of the PMT channel of module LBA23. An improvement up to 20% is observed with respect to the RMS obtained before applying the χ^2 method. Significant improvements associated to channels which have shown important correlation effects are noticeable. As an example, in Figure 8 the changes observed for PMT 46 (left) and PMT 20 (right), from the LBA23 module, are shown.

The values of the α matrix can be observed in Figure 9 (left) together with the offset values (β_i) in the diagonal. It can be seen that, as expected, the matrix reflects the configuration of the TileCal

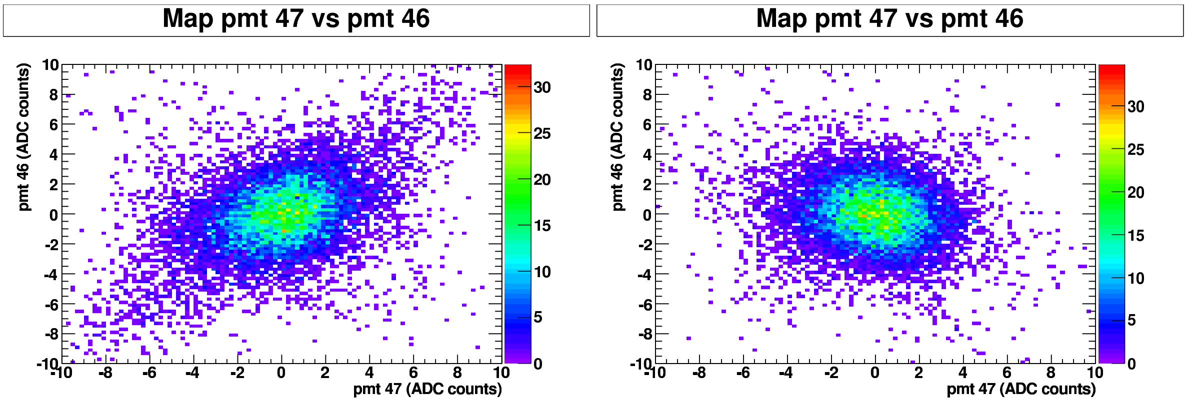

Figure 5: The pedestal from PMT 47 is plotted against the one from PMT 46 before (left) and after (right) removing the correlated noise component with the χ^2 method.

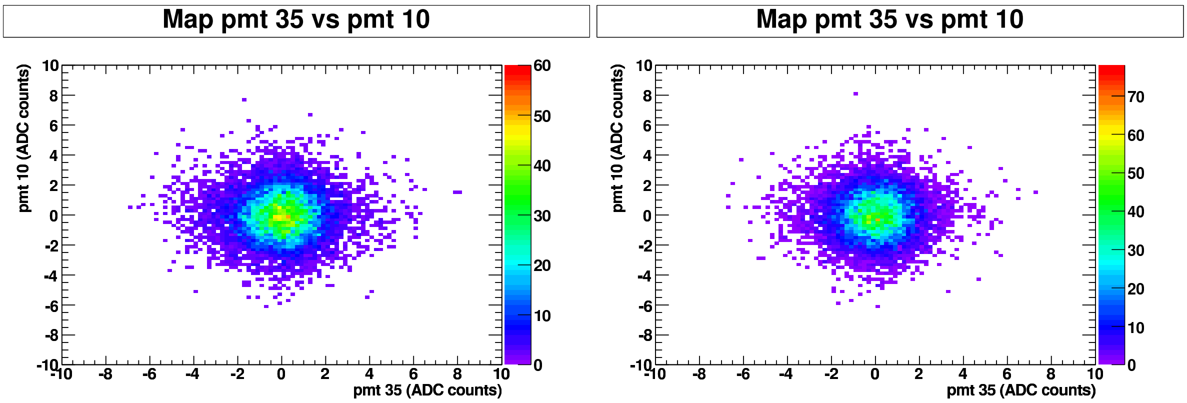

Figure 6: The pedestal from PMT 35 is plotted against the one from PMT 10 before (left) and after (right) removing the correlated noise component with the χ^2 method.

hardware with clear clusters of neighbour channels determining the PMT signal responses. The offset values are also close to zero, as expected. In Figure 9 (right) the covariance values, $cov(i, j)$ between the different PMTs of module LBA23 are shown, not including the diagonal terms. The red and blue lines represent the covariance before and after removing the correlations. Once more the improvement in the covariance values is noticeable after applying the χ^2 method. It is also interesting to remark the existence of negative values of the covariance which suggests the persistence of an anti-correlation component even after applying the χ^2 method. Its source needs further investigation.

A word on the double Gaussian fit of the pedestal distributions is due here: although removing the correlated noise improves the general behaviour of the PMTs, the need for a double Gaussian function is not ruled out. In Figure 10, the fit of PMT 45 distribution before and after applying the χ^2 method shows that the fit improves after removing the correlated noise (with a better reduced χ^2) but the second Gaussian is still necessary. And this occurs in spite of the amplitude of the second Gaussian being reduced i.e., its importance decreased, and the width of the dominant Gaussian was also reduced.

In Figures 11 and 12 examples of two-dimensional covariance matrices for other modules of the TileCal (LBA38 and LBC26) are shown. The distributions show a similar pattern when compared with the LAB23 module studied above i.e., the correlations are reduced to a large extent by applying the χ^2 method.

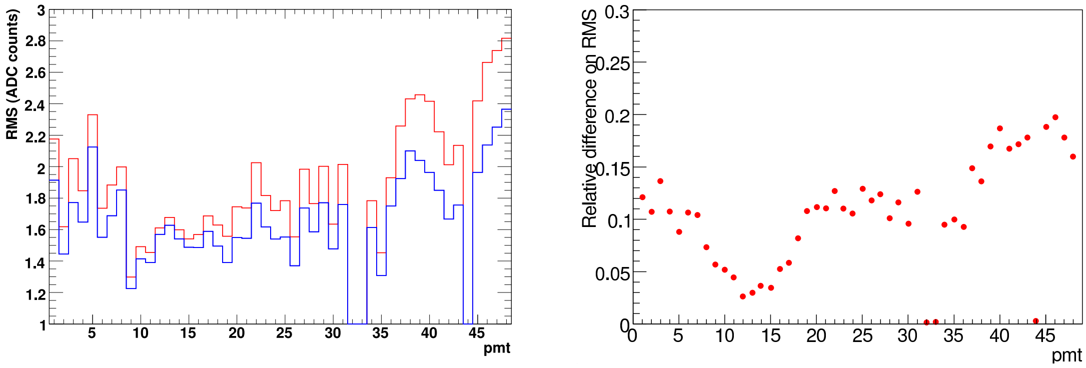

Figure 7: The distribution of the noise RMS is shown for all channels of the LBA23 TileCal module. Left: the top (red) and bottom (blue) lines correspond to the values obtained before and after applying the χ^2 method, respectively. Right: the relative change of the RMS is represented as a function of the PMT channel of module LBA23.

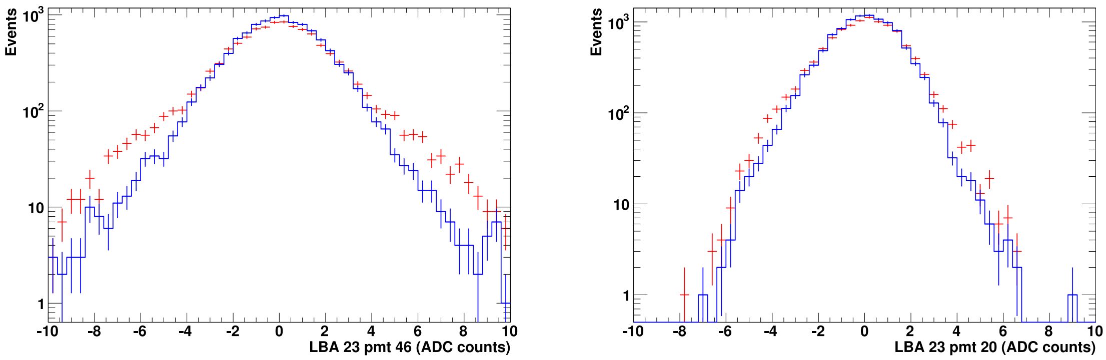

Figure 8: Left: the PMT 46 of the TileCal LBA23 module is shown before (red dots) and after (blue line) applying the χ^2 method. Right: the PMT 20 of the TileCal LBA23 module is shown before (red) and after (blue) applying the χ^2 method.

6 Conclusion

A new method to remove the correlated noise component of the TileCal has been proposed. The method is based on a simple χ^2 minimization and its performance was successfuly tested using TileCal pedestal runs in the high gain read-out. Although the work focused on the module LBA23, other modules were also tested with similar results. The method is efficient in removing the correlated noise contribution that affects the TileCal PMTs and improves the RMS of pedestals by up to 20%. Although the double Gaussian structure of the pedestals is more constrained after applying the χ^2 method and removing the noise correlations, its not completely ruled out. This suggests that the source for the remaining double Gaussian structure of the pedestals is different from the correlated noise itself within the module, and needs further investigation. A full and systematic survey of the TileCal modules is still to be done in a near future.

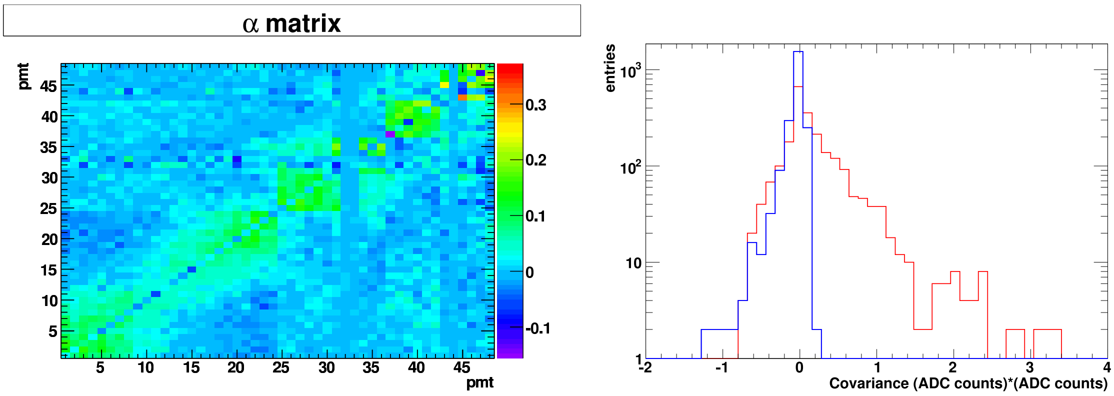

Figure 9: Left: the α matrix is represented together with the β_i offsets in the diagonal. Right: the covariance values, $cov(i, j)$ between the different PMTs of module LBA23 is shown, not including the diagonal terms ($i = j$). The red and blue lines represent the covariance before and after removing the correlations.

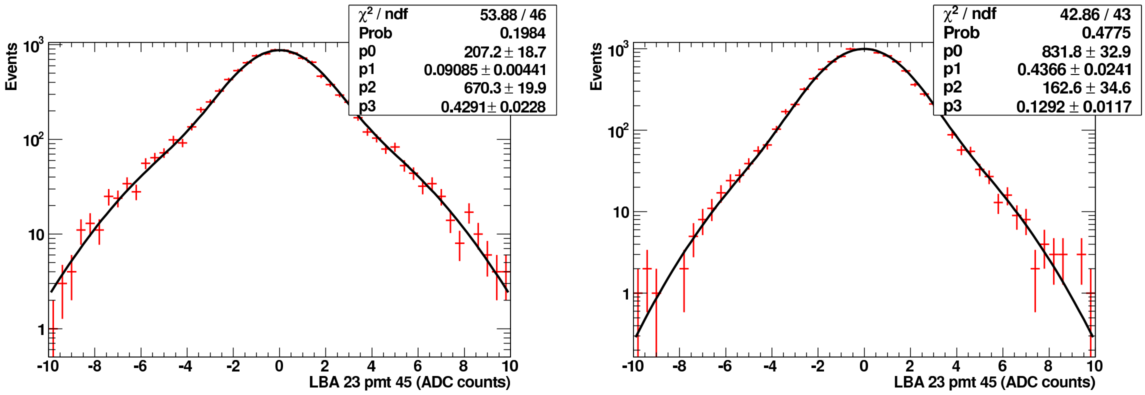

Figure 10: The fit of the PMT 45 distribution with a double Gaussian function is shown before (left) and after (right) applying the χ^2 method.

7 Acknowledgements

The work of M.C.N. Fiolhais has been supported by Fundação para a Ciência e Tecnologia (FCT), grant SFRH/BD/48680/2008. The authors would like to specially thank João Carvalho and Nuno Castro for their careful reading of the manuscript, suggestions and comments. Sasha Solodkov and Luca Fiorini are greatly aknowledged by their invaluable help and continuous support during the development of this work. Special thanks are due to Ana Henriques and Irene Vichou for all discussions and suggestions specially during the ATLAS Overview Week 2009 which reflected in the current write up.

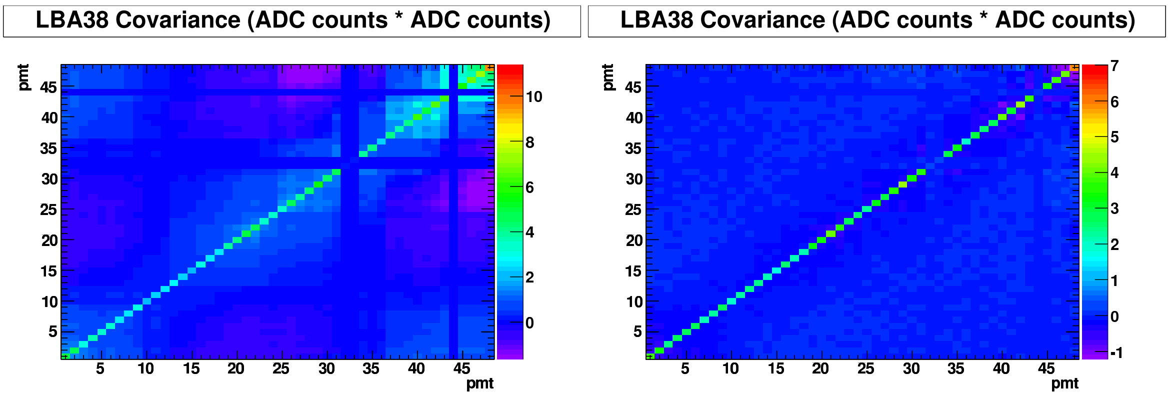

Figure 11: The two dimensional covariance matrix, in (ADC counts)^2, is represented for the LBA38 module of the TileCal before (left) and after (right) removing the correlated noise distribution

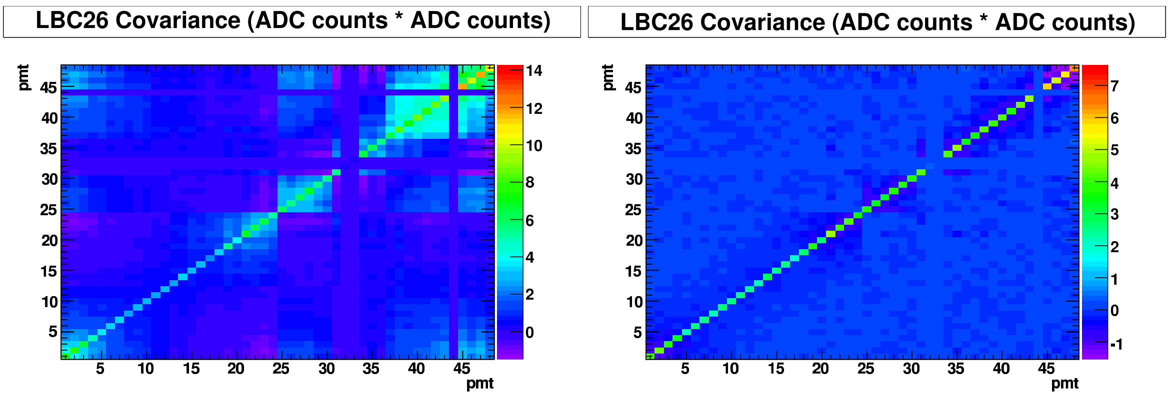

Figure 12: The two dimensional covariance matrix, in (ADC counts)^2, is represented for the LBC26 module of the TileCal before (left) and after (right) removing the correlated noise distribution

References

[1] G.Aad *et al.*, ATLAS Collaboration, *"The ATLAS Experiment at the CERN Large Hadron Collider"*, JINST **3** S08003 (2008).

[2] ATLAS Tile Calorimeter Collaboration, *"Tile Calorimeter Technical Design Report"*, CERN/LHCC/96-42 (1996).

[3] T. Stelzer, Z. Sullivan and S. Willenbrock, Phys. Rev. D **58** (1998) 094021

[4] F. Spanò, ATL-TILECAL-PUB-2008-011, 30 October 2008.